

## Influence of the Supporting Material on the Conical Monopole Sensor Calibration Setup

Hamad. A. Deiban<sup>(1)</sup>, Fernando Albarracin<sup>(1)</sup>, and Chaouki Kasmi<sup>(1)</sup>

(1) Directed Energy Research Center, Technology Innovation Institute, Abu Dhabi, United Arab Emirates; e-mail: Hamad.Deiban@tii.ae

### Abstract

In this paper the influence of the supporting material on the electric response of the conical-monopole-based sensor calibration setup is analyzed and presented. The analysis is supported by numerical simulations and measurements of the impedance response. The electric field in the region of influence is also calculated. Two different use cases for the base support of the conical monopole are presented as a comparative analysis.

### 1 Introduction

In many High-Power Microwave and Pulsed Power applications measuring electromagnetic environments is an important task in both characterizing the source or in studying its effects in other systems [1]. In recent decades such measurement is enabled using two types of sensors, they are B-dot and D-dot, representing magnetic and electric field sensors, respectively. Both are voltage time derivative devices which depend ultimately on the constructed sensing area which field passes through. In other words, these sensors are represented by a transfer function across certain frequency range depending on their geometry. One of the approaches to calibrate such sensors is by using a ground plane setup with conical monopole antenna [2] as shown in Figure 1:

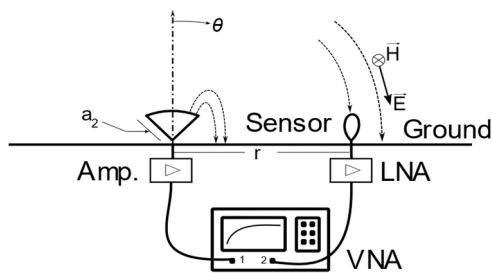


**Figure 1.** Ground Plane calibration setup, presented by the authors in [2].

In an ideal setup the conical monopole is placed perpendicular on the ground plane with distance  $r$  from the sensor under test. The monopole is designed as discussed in [2] and [3] to maintain an impedance of  $50 \Omega$  to match the measurement system impedance, in this case, the Vector Network Analyzer, VNA.

Papas & King in [4] derived a solution for estimating the conical monopole impedance with a length  $a_2$  and flare

angle  $\theta_0$  (see Figure 2 (a) as a reference), computed as in equation (1)

$$Z_c = Z_0 \frac{1 - \beta/\alpha}{1 + \beta/\alpha}; \quad Z_0 = 60 \ln \cot \frac{\theta_0}{2} \quad (1)$$

where  $Z_0$  is the characteristic impedance of the conical transmission line antenna, and  $\frac{\beta}{\alpha}$  is the ratio of the propagating TEM waves amplitude in the antenna region.  $\alpha$  and  $\beta$  are computed as combinations of the Legendre polynomials and the spherical Hankel functions of the second kind [4].

The electric field radiated by the conical monopole, close to the ground plane (i.e.,  $\theta = 90^\circ$  in Figure 1), can be computed as in equation (2) [3]:

$$E_\theta = V_{in} \frac{Y_{in}}{f} \frac{a_2}{4\pi} \eta_0 \left( j \frac{2\pi f^2}{c_0 r} + \frac{f}{r^2} - j \frac{c_0}{2\pi r^3} \right) e^{-j2\pi r f / c_0} \quad (2)$$

where  $Y_{in} = 1/Z_c$  is the conical monopole admittance,  $f$  is the frequency range,  $r$  is the sensor distance from the conical monopole,  $a_2$  is the conical monopole slant length,  $\eta_0$  is the free space impedance, and  $c_0$  is the speed of light. The spectral analysis of the conical monopole over a ground plane, when utilized as a sensor calibration setup was presented by the authors in [5].

### 2 Implementation of the Conical Monopole as a Calibration Setup

The design and implementation details of a conical monopole for sensor calibration along with the implementation over a realistic ground plane to compose an EM sensor calibration setup is presented in this section. The conical geometry with a flare angle,  $\theta_0 = 47^\circ$ , i.e., corresponding to a system impedance of  $50 \Omega$ , and an apothem  $a_2 = 40$  mm, is shown in Figure 2 (a). A prototype of the monopole, integrated with a  $2.4 \times 2.4$  m<sup>2</sup> stainless steel ground plane was fabricated and tested in a semi-anechoic chamber in the Technology Innovation Institute, TII, labs. The prototype was made with solid brass with tin coating. A detailed picture of the prototype is shown in Figure 2 (b). A 3D-printed resin base is used to support the cone in place. A RG405, 20 mm length, RF cable section is used to feed the setup. The analytical impedance of the monopole is shown in Figure 3. The ideal full-wave simulated response, i.e., with the conical monopole ideally fed from the apex is also shown.

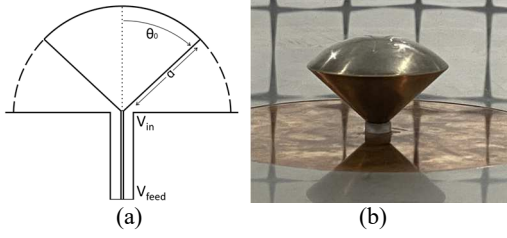


**Figure 2.** Conical Monopole: (a) geometry scheme, and (b) implemented prototype on a resin base.

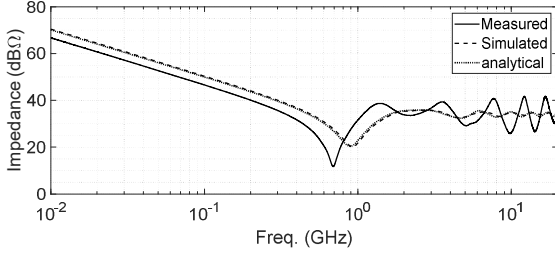


**Figure 3.** Conical Monopole impedance response. The measured results correspond to the implementation with a resin support base.

The first minimum of the impedance response,  $Z_c$ , is around 950 MHz, as the analytical and simulated curves shown in Figure 3. The measured response shows similar behavior but shifted to lower frequencies, with the first minimum in 600 MHz. At a first glance, the dielectric support base, whose permittivity is expected to be higher than that from the air, is the cause of the measured response.

### 3 Impedance Response Analysis

#### 3.1 Modelling the dielectric support-base

The electric field expression in (2) assumes the voltage excitation in the apex of the cone. In the practical implementation of the conical monopole, as the one presented here, a coaxial transmission line (TL) section and the support base of the cone contribute to an attenuation and phase shifting in the applied voltage signal,  $V_{feed}$  in Figure 2 (a). This effect must be considered since an accurate electric field expression shall be used to effectively calibrate an electromagnetic sensor using this calibration setup.

The scheme in Figure 4 shows the system view to compute the voltage  $V_{in}$ . Two cascaded S-parameters matrices, representing the coaxial TL and the resin base, respectively.

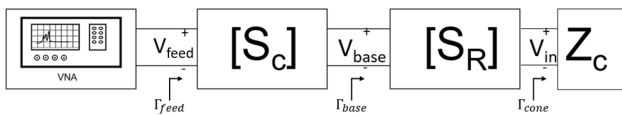


**Figure 4:** Two-Port Network of the Conical Monopole with supporting material.

The first section,  $[S_C]$ , can be modeled as a low loss transmission line, with characteristic impedance,  $Z_0 = 50 \Omega$ , length  $l_1$ , and propagation constant  $\beta_1$ . The second section,  $[S_R]$  represents a conical TEM transmission line, with a length  $l_2$ , propagation constant  $\beta_2$ , and characteristic impedance  $Z_R$  computed as in equation (3):

$$Z_R = \frac{60}{\sqrt{\epsilon_r}} \ln \left( \cot \frac{\theta_0}{2} \right) \quad (3)$$

where  $\epsilon_r$  is the permittivity of the resin and  $\theta_0$  is the flare angle of the conical monopole. Note that  $l_2$  equals the apothem of the cone covered by the resin base.

The voltage transfer function of the cascaded  $[S_C]$  and  $[S_R]$  sections, i.e.  $V_{in}/V_{feed}$ , can be computed as in equation (4)

$$\frac{V_{in}}{V_{feed}} = \frac{V_{in}}{V_{base}} \frac{V_{base}}{V_{feed}} = \frac{S_{R,21}(1+\Gamma_{cone})(1+\Gamma_{base})(1+\Gamma_{feed}) \exp(-j2\pi f \cdot l_1 \sqrt{\epsilon_{r,TL}} (c_0^{-1}))}{(1-S_{R,22}\Gamma_{cone})(1+S_{R,11})+S_{R,12}S_{R,21}\Gamma_{cone}} \quad (4)$$

Note that the coaxial TL contribution is included in the term  $(1+\Gamma_{feed}) \exp(-j2\pi f \cdot l_1)$ . The resin-based TL section has a characteristic impedance  $Z_R$ . The response of the electric field, normalized to the feed voltage,  $TF_{CS}$  within the influence area of the calibration setup, including the feed path correction can be calculated by placing (4) into (2):

$$TF_{CS} = \frac{E_0}{V_{feed}} = \left[ \frac{S_{R,21}(1+\Gamma_{cone})(1+\Gamma_{base})(1+\Gamma_{feed}) \exp(-j2\pi f \cdot l_1 \sqrt{\epsilon_{r,TL}} (c_0^{-1}))}{(1-S_{R,22}\Gamma_{cone})(1+S_{R,11})+S_{R,12}S_{R,21}\Gamma_{cone}} \right] \quad (5)$$

$$\left[ \frac{Y_{in}}{f} \frac{a_2}{4\pi} \eta_0 \left( j \frac{2\pi f^2}{c_0 r} + \frac{f}{r^2} - j \frac{c_0}{2\pi r^3} \right) e^{-j2\pi f r / c_0} \right]$$

where  $V_{feed}$  is the voltage at the feed point of the setup in Figure 4,  $S_{R,21}$  and  $S_{R,22}$  are the forward gain and reflection of the supporting base output, respectively, the  $S_{R,11}$  and  $S_{R,12}$  are the reflection and reverse gain at the base input, respectively.  $\Gamma_{cone}$ , and  $\Gamma_{base}$   $\Gamma_{feed}$ , are the reflection coefficients of the conical monopole, the supporting resin base, and the coaxial TL respectively.

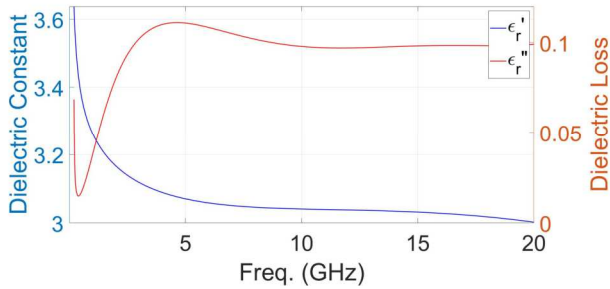
#### 3.2 Characterization of the supporting base material

The next step in the response analysis is the characterization of the dielectric parameters of the epoxy resin used for the conical monopole base. An instrumented open-ended coaxial probe, connected to a VNA were used, as shown in Figure 5 (a). The real and imaginary parts of the electric permittivity,  $\epsilon'$  and  $\epsilon''$ , normalized to  $\epsilon_0$ , have been measured up to 20 GHz for a parallelepipedal sample of the epoxy resin. The results are shown in Figure 5 (b). As expected, the real relative permittivity value is between 3 and 3.5. The values of  $\epsilon''$  indicate low dielectric losses in

the material, validating the low-loss transmission line analysis presented above.



(a)



(b)

**Figure 5.** (a) Measurement setup with DAK system. (b) Resin measured relative dielectric permittivity

Using the obtained results from the dielectric material characterization, a transmission line model of the resin-TL section was simulated using the CST circuit simulator. The extracted  $[S_R]$  matrix was then cascaded with the coax TL section,  $[S_C]$ , and finally, connected to the ideally fed conical monopole. The input impedance response of the setup is shown in Figure 6 where the blue curve represents the simulated setup and the red curve the measurement. The agreement between the measured and the simulated setup indicates that the analysis in Section 3.1 is correct.

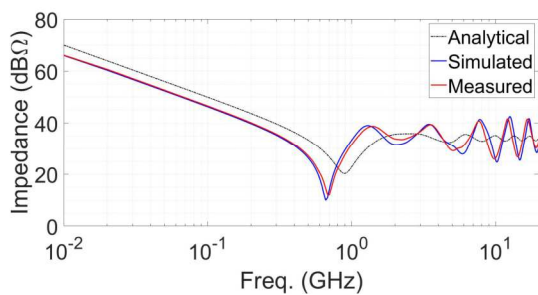


**Figure 6.** Comparison between the analytical, simulated, and measured impedance response including the resin effect.

Finally, the calibration setup transfer function  $TF_{CS}$  is computed, using the compensated expression in (5). The results are shown in Figure 7. The value of  $TF_{CS}$  for frequencies higher than 500 MHz differ in more than 3 dB from the analytical value in (2). This compensated  $TF_{CS}$  expression must be used during the electromagnetic sensor calibration process.

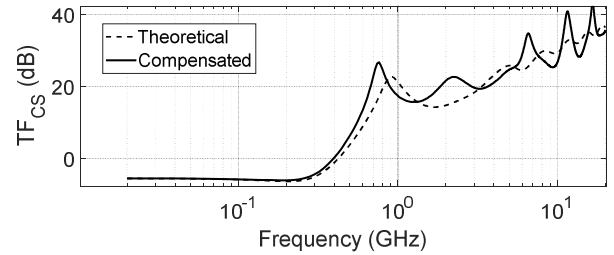


**Figure 7.** Electric Field comparison between Theoretical and Compensated electric field at a distance  $r = 150$  mm.

#### 4 Alternative base support design

An alternative solution to the distorted response of  $Z_c$  due to the epoxy resin base is presented in this section. A low loss, low permittivity material, the rohacell HF31®, with a permittivity,  $\epsilon_r \sim 1.07$ , is characterized. A crown shaped support has been designed and simulated in CST studio. The proposed geometry is shown in Figure 8. For comparison purposes, the same resin-based geometry was simulated, this time using rohacell material. The impedance response is shown in Figure 9 for both rohacell-based support geometries. One important advantage of the ring support is that visual inspection of the apex connection to the coaxial feed is enabled. Although the minimum of the impedance magnitude is also shifted toward lower frequencies with the rohacell supports, the high frequency response fits better the analytical impedance  $Z_c$ .

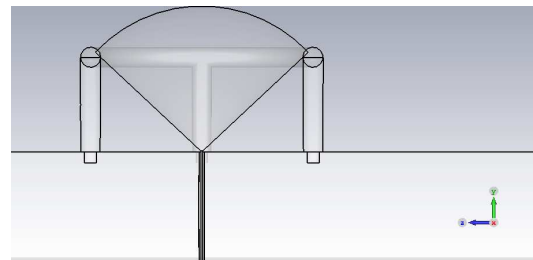


**Figure 8.** Conical monopole with crown support (in white)

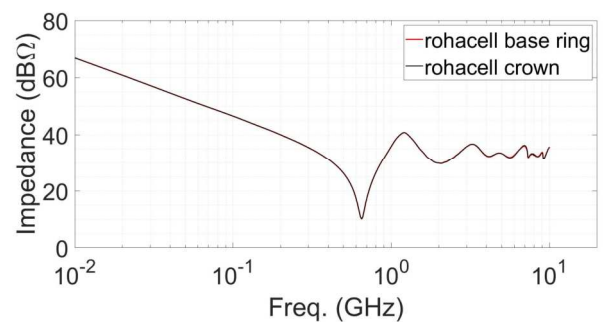


**Figure 9.** Conical Monopole impedance using ring and crown shaped supports.

## 5 Conclusion

The practical implementation of an electromagnetic sensor calibration setup, based on a compact conical monopole over a ground plane, has been presented. The challenges in understanding the disagreement between the theoretical and the measured values for the impedance response have been addressed by using a low-loss transmission line model analysis. A compensation to the transfer function,  $E_{\theta} / V_{feed}$ , has been derived for future measurements and calibration procedures. An alternative geometry for the monopole support has been proposed. Simulated results are promising. In this alternative design a material with dielectric constant close to air can limit the disturbance in the impedance response. The resulting performance of the conical monopole impedance using the rohacell as stabilizing material will be carried out in the future measurements.

## References

- [1] C. Baum, E. Breen, J. Giles, J. O'Neill, and G. Sower, "Sensors for Electromagnetic Pulse Measurements Both Inside and Away from Nuclear Source Regions," *IEEE Trans. Electromagn. Compat.*, vol. EMC-20, no. 1, pp. 22–35, Feb. 1978, doi: 10.1109/TEMC.1978.303690.
- [2] F. Albarracin, D. Martinez, G. N. Appiah, J. Galvis, C. Kasmi, and N. Mora, "Spectral Response of the Conical Monopole as Field Sensor Calibration Setup," *IEEE Lett. Electromagn. Compat. Pract. Appl.*, vol. 4, no. 2, pp. 47–51, Jun. 2022, doi: 10.1109/LEMCPA.2022.3157484.
- [3] F. Bieth and P. Delmote, "Calibration With a Monocone on a Ground Plane," *IEEE Trans. Plasma Sci.*, vol. 45, no. 10, pp. 2744–2747, Oct. 2017, doi: 10.1109/TPS.2017.2703877.
- [4] C. H. Papas and R. King, "Input Impedance of Wide-Angle Conical Antennas Fed by a Coaxial Line," *Proc. IRE*, vol. 37, no. 11, pp. 1269–1271, Nov. 1949, doi: 10.1109/JRPROC.1949.234607.
- [5] F. Albarracin-Vargas, D. Martinez, G. N. Appiah, J. Galvis, C. Kasmi, and N. Mora, "Spectral Response of Electromagnetic Field Sensor Calibration Setups," in *2021 IEEE International Joint EMC/SI/PI and EMC Europe Symposium*, Raleigh, NC, USA, Jul. 2021, pp. 131–131. doi: 10.1109/EMC/SI/PI/EMCEurope52599.2021.9559329.